

# Elemental mapping of spinodal decomposition in duplex stainless steels

T Yamada<sup>1</sup>, J M Titchmarsh<sup>2</sup>, R E Dunin-Borkowski<sup>3</sup> and S Lozano-Perez<sup>2</sup>

<sup>1</sup> INSS, 64 Sata, Mihama-cho, Makata-gun, Fukui 919-1205, Japan

<sup>2</sup> Department of Materials, Parks Road, Oxford OX1 3PH

<sup>3</sup> Department of Materials Science and Metallurgy, Pembroke Street, Cambridge CB2 3QZ

**ABSTRACT:** Spinodal decomposition (SD) in a duplex stainless steel, exposed to different heat treatments, has been examined using both energy-filtered transmission electron microscopy (EFTEM) in a Gatan Imaging Filter (GIF) and energy dispersive X-ray (EDX) spectroscopy. It was found that the EFTEM Cr and Fe maps were of consistently higher contrast than the EDX maps and could be used routinely to determine the dimensions of the decomposition.

## 1. INTRODUCTION

At temperatures above 300°C, regions of delta ferrite in duplex stainless steels are susceptible to SD (Cottrell, 1995), which involves phase separation into Fe-rich and Cr-rich regions and can result in the embrittlement of austenitic castings and welds (Vitek et al., 1991). The time and temperature dependence of SD have traditionally been characterised using the position sensitive atom probe (PoSAP) (e.g. Brown et al., 1990) because the scale of the SD has been considered too small for TEM-based analytical techniques. Here, we assess the degree to which EFTEM and EDX can reveal the Cr and Fe distributions in a duplex stainless steel that has been aged at two temperatures for various times.

## 2. EXPERIMENTAL DETAILS

Duplex stainless steel samples of approximate composition  $\text{Fe}_{63}\text{Cr}_{22}\text{Ni}_9\text{Si}_2\text{Mo}_3\text{Mn}_1$  were heat-treated at 450°C for 50 hrs, 400°C for 1000 hrs, 400°C for 300 hrs and 400°C for 3000 hrs (Samples 1-4, respectively). TEM specimens were prepared by electropolishing with 5% perchloric acid in ethanol. EFTEM images (Egerton, 1996) were obtained at 300 kV using JEOL JEM-3000F ( $C_s = 0.6$  mm,  $C_c = 1.3$  mm) and Philips CM300-ST ( $C_s = 1.2$  mm,  $C_c = 1.5$  mm) field emission gun TEMs. Both microscopes are equipped with GIFs with 2k CCD cameras and were operated at magnifications of between x10k and x20k. EDX maps were collected at 100 kV in a VG HB501 scanning TEM using an Oxford Instruments windowless EDX detector. A probe diameter of ~2 nm (full width at half maximum) and a pixel size of ~0.8 nm were used as a compromise between signal intensity and spatial resolution. Contamination present on some samples was removed by plasma cleaning, while etching in others was overcome by depositing a very thin layer of carbon.

### 3. RESULTS

EFTEM image resolution and contrast were explored systematically by varying the size of the objective aperture and both the position and the width of the energy windows. The locations of the selected 20eV wide windows are shown in Fig. 1a. Although a theoretical optimum objective aperture semi-angle of 4.1 mrad was derived using the method of Krivanek et al. (1995) (Fig. 1b), the predicted resolution was considered to be pessimistic and the intensity of the signal was low. A 12.2 mrad aperture was found to provide adequate resolution with acceptable intensity for image acquisition times of between 20 and 40 s.

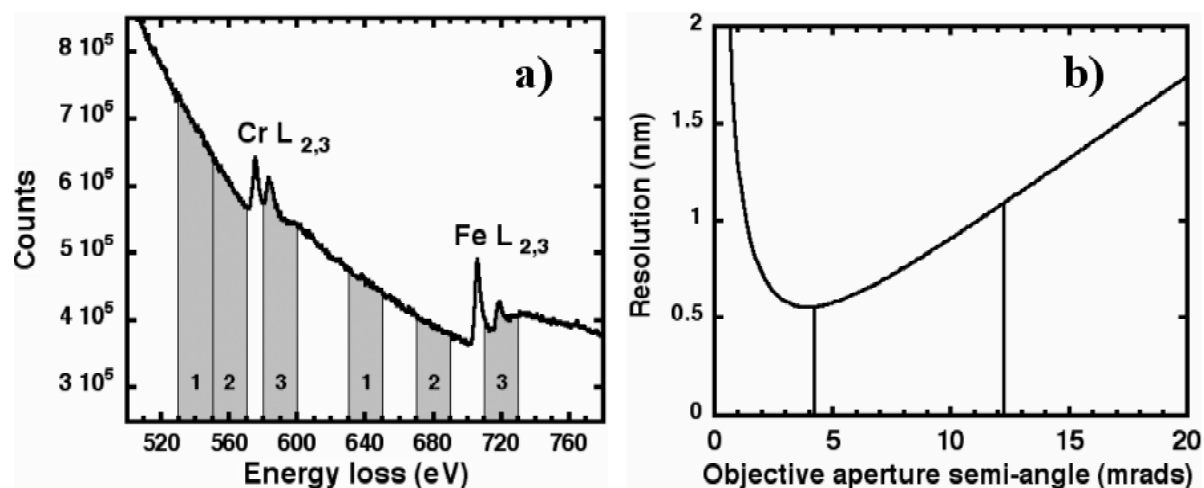


Fig.1. a) Electron energy-loss spectrum obtained from a region of delta ferrite in Sample 1. Windows used for 3-window elemental mapping are marked; b) Predicted resolution of images obtained at 580 eV loss using a 20 eV wide energy-selecting slit in a JEOL JEM-3000F at 300 kV, following Krivanek et al. (1995). The 4.1 and 12.2 mrad collection aperture semi-angles available experimentally are marked by vertical lines.

A representative series of EFTEM images and three window background-subtracted elemental maps from Sample 1 is shown in Fig. 2. For each sample, between 5 and 20 such sets were recorded across a 60nm-wide field of view. The greater contrast observed in the Cr maps is due to the larger relative changes in Cr concentration and the larger Cr-L<sub>23</sub> edge ionisation cross section, as compared with that of Fe. Examples of Cr maps from the four samples are shown in Fig. 3. The periodicity of the SD image contrast was derived by 2D-autocorrelation analysis, giving average values for Samples 1-4 of 6.5, 4.7, 2.5 and 4.7 nm, respectively. The application of a 2D-autocorrelation function to the projection of a 3D structure will yield progressively smaller (and more erroneous) values as the foil thickness increases, due to feature overlap. Tomographic ( $\pm 60^\circ$  tilt) work is presently being developed to generate 3D chemical information for direct comparison with PoSAP analysis. Even so, the present 2D results demonstrate a consistent trend with heat treatment temperature and time.

Although small, significant variations in Cr:Fe concentration ratio were observed when acquiring EDX spectra using random probe positions (Fig. 4), considerable difficulties were encountered when generating EDX elemental maps. The need to map the very thin edges of the specimens to prevent potential overlap of features resulted in very low counting rates and low signal-to-noise ratios, sometimes with large variations of thickness across the map (Fig. 5). Image acquisition times in excess of 30 minutes were required, sometimes resulting in distortion and loss of feature definition as a result of specimen drift. The scale of the SD in Samples 2 and 3 was too small to reveal clearly and 2D-autocorrelation analysis of EDX maps was not attempted.

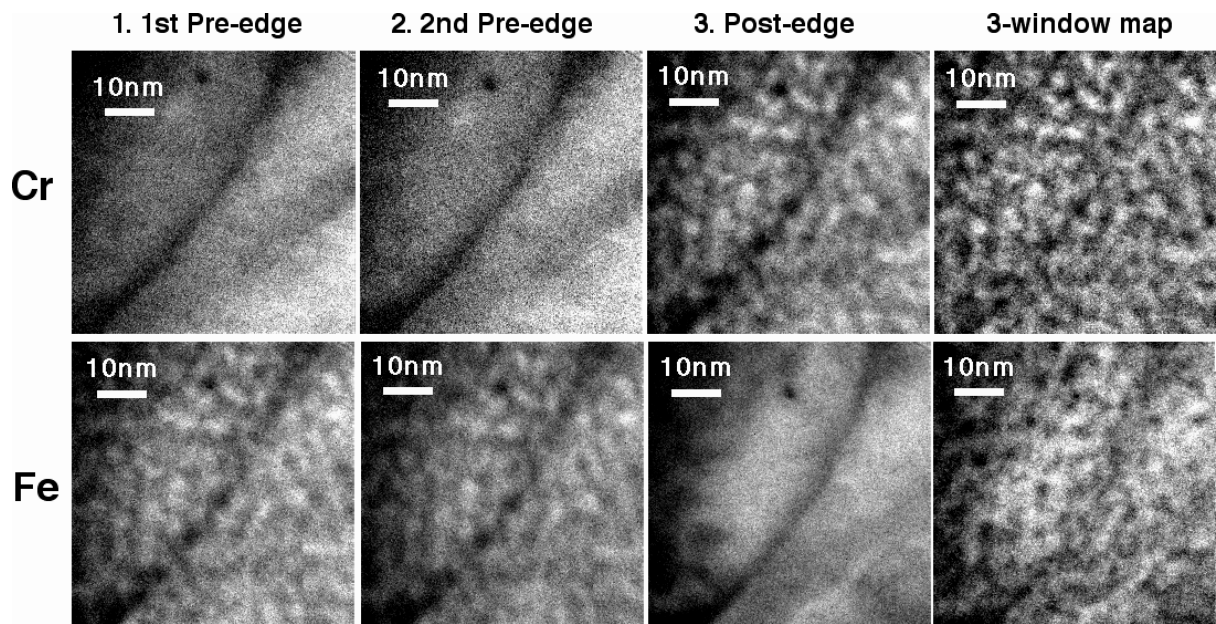


Fig. 2. Cr and Fe energy-selected images obtained from a region of delta ferrite in Sample 1 using windows labelled in Fig. 1. 3-window maps were formed by using the pre-edge images to calculate a power-law background, which was then subtracted from the post-edge image.

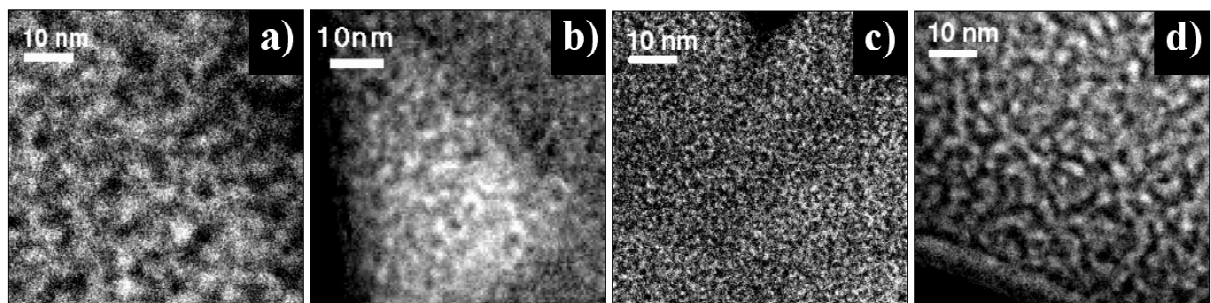


Fig. 3. a) – d) Cr 3-window maps obtained from delta ferrite in Samples 1 - 4, respectively.

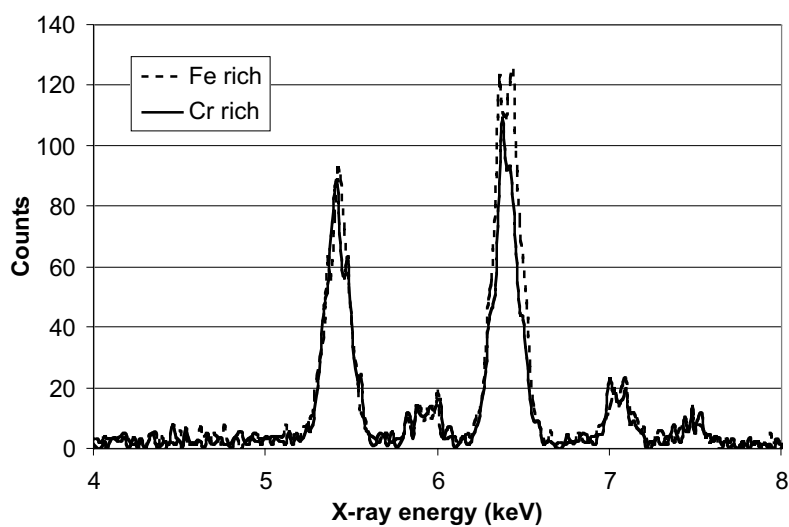


Fig. 4. EDX spectra from Sample 4, which have been scaled at the Cr  $K_{\alpha}$  peak.

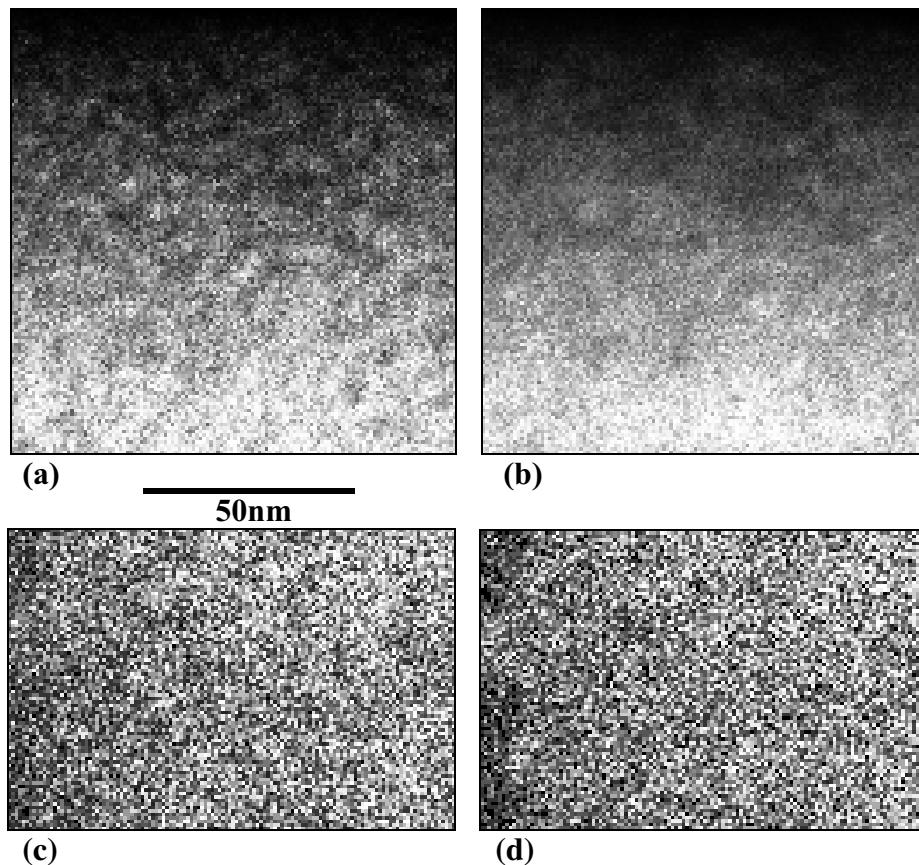


Fig. 5 EDX elemental maps: (a) Cr and (b) Fe (Sample 2), and (c) Cr and (d) Fe (Sample 4).

#### 4. CONCLUSIONS

Both GIF and EDX elemental mapping have been used to reveal the presence of SD compositional fluctuations in aged cast austenitic steel. The results from GIF mapping were found to be superior to those from EDX. GIF mapping revealed clear and consistent variations in the scale of SD. Spatial quantification is possible providing the foil thickness is not large enough to cause significant feature overlap. GIF mapping is a rapid and accurate method for the investigation of SD that will rival PoSAP as a characterisation tool when it is combined with electron tomography to provide 3D chemical information.

#### ACKNOWLEDGMENTS

The authors are grateful for support from INSS (JMT and SL-P) and the Royal Society (RED).

#### REFERENCES

- Brown JE, Cerezo A, Godfrey TJ, Hetherington MG, Smith GDW 1990, *Mat. Sci. Tec.* **6**, 129
- Cottrell AH 1995 *An Introduction to Metallurgy* (Institute of Metals, London)
- Egerton RF 1996 *Electron Energy-Loss Spectroscopy in the Electron Microscope* (Plenum, New York)
- Krivanek OL, Kundmann MK and Kimoto K 1995 *J. Microsc.* **180**, 277
- Vitek JM, David SA, Alexander DJ, Keiser JR and Nanstad RK 1991 *Acta Metall. Mater.* **39**, 503